ELSEVIER

Journal of Alloys and Compounds 431 (2007) 56–64

Journal of ALLOYS AND COMPOUNDS

www.elsevier.com/locate/jallcom

The influence of Cd-dopant on the properties of α-FeOOH and α-Fe_2O_3 particles precipitated in highly alkaline media

Stjepko Krehula, Svetozar Musić *

Division of Materials Chemistry, Ruđer Bošković Institute, P.O. Box 180, HR-10002 Zagreb, Croatia

Received 11 May 2006; received in revised form 18 May 2006; accepted 20 May 2006
Available online 30 June 2006

Abstract

The effects of Cd-dopant on the phenomenology of the precipitation of α-(Fe, Cd)OOH and α-(Fe, Cd)$_2O_3$ particles, the formation of solid solutions, particle size and their geometrical shapes were investigated using Mössbauer and Fourier transform infrared (FT-IR) spectroscopies, field emission scanning electron microscopy (FE SEM) and energy dispersive X-ray analysis (EDS). The formation of merely α-(Fe, Cd)OOH solid solutions was measured up to $r = 0.0196$, where $r = [Cd]/([Cd] + [Fe])$. The formation of two types of solid solutions, α-(Fe, Cd)OOH and α-(Fe, Cd)$_2O_3$ was found at r between 0.0291 and 0.0698, whereas the formation of an α-(Fe, Cd)$_2O_3$ solid solution alone was obtained at $r = 0.0909$. The incorporation of Cd-substitutions into α-FeOOH and α-Fe_2O_3 structures decreased the $\langle B_{hf} \rangle$ values of the corresponding hyperfine magnetic field. The IR band at 639 cm^{-1}, recorded for α-FeOOH, was found to be sensitive to Cd-substitutions. With an increased r value a gradual elongation of α-(Fe, Cd)OOH particles along the c-axis was observed, with the maximum elongation (∼600–700 nm) obtained at $r = 0.0476$. At the same time, particle width (b-axis direction) and thickness (a-axis direction) showed a gradual decrease. With a further increase in the r value the length of α-(Fe, Cd)OOH particles rapidly decreased. α-(Fe, Cd)$_2O_3$ particles ∼100–200 nm in size were obtained at $r = 0.0909$.

Keywords: Cadmium; Tetramethylammonium hydroxide; α-FeOOH; α-Fe_2O_3; ^{57}Fe Mössbauer; FT-IR; FE SEM; EDS

1. Introduction

The influence of various metal cations on the precipitation of *iron oxides* (group name for iron-oxyhydroxides and -oxides) has been the subject of many investigations. In these studies researchers were mainly focused on α-FeOOH (goethite) and α-Fe_2O_3 (hematite). These compounds are the constituents of many soils and for that reason it is important to have knowledge about the incorporation of "foreign" metal cations into their crystal structure. α-FeOOH and α-Fe_2O_3 can also be scavengers for various metal cations of high toxicity, as well as for many radionuclides. Natural α-FeOOH may contain a significant amount of substituted metal cations which can be preconcentrated in metallurgy for their commercial production in a pure metallic state.

The investigation of the effects of various metal cations on the precipitation of *iron oxides* and the formation of solid solutions is also important from an academic standpoint. In these investigations α-FeOOH and α-Fe_2O_3 were mainly used as model systems. The incorporations of metal cations in the crystal structures of α-FeOOH and α-Fe_2O_3 were determined using classical chemical analyses, X-ray diffraction (XRD) or Mössbauer spectroscopy. In these investigations the Mössbauer spectroscopy has advantage over the XRD technique when the radii of metal cations are very close to ionic radius of Fe^{3+}, for example, in the case of Ni^{2+} or V^{3+}. Also, Mössbauer spectroscopy is more sensitive and accurate than XRD in determination of α-FeOOH and α-Fe_2O_3 mixed phases in the precipitates. Specifically, this is pronounced if the fraction of α-FeOOH is significantly higher than that of α-Fe_2O_3 and vice versa.

In the present work, we have focused on the influence of Cd-dopant on the properties of α-FeOOH and α-Fe_2O_3 particles precipitated in highly alkaline media. The knowledge about the formation of solid solutions with Cd^{2+} ions is also practically important. Cadmium is a highly toxic metal which can be the source of pollution in some industries, for example in battery factories, zinc smelters or pigment plants or during some soldering activities. Also, cadmium gets into the soil from fertilisers or

* Corresponding author.
E-mail address: music@irb.hr (S. Musić).

0925-8388/$ – see front matter © 2006 Elsevier B.V. All rights reserved.
doi:10.1016/j.jallcom.2006.05.081

via discharge in zinc-mining processes. Cadmium toxication via the food chain becomes a growing concern. The major source of cadmium is cigarette smoke which is toxic for smokers and nonsmokers alike. Environmental and occupational exposure to cadmium can cause renal dysfunction, bone disease and possibly cancer.

The aim of the present work has been to investigate: (a) the influence of Cd^{2+} concentration on the formation of α-FeOOH and α-Fe_2O_3 particles in highly alkaline media, (b) the formation of solid solutions α-(Fe, Cd)OOH and α-$(Fe, Cd)_2O_3$ and (c) the effect of Cd^{2+} ions on the size and morphology of the particles precipitated. In the present work, we analysed the synthesized samples using Mössbauer spectroscopy, FT-IR, FE SEM and EDS. To our best knowledge, the influence of Cd-dopant on the properties of α-FeOOH and α-Fe_2O_3 precipitates has not been previously investigated by Mössbauer spectroscopy.

2. Experimental

2.1. Preparation of samples

Chemicals of analytical purity, $FeCl_3 \cdot 6H_2O$, supplied by Kemika, and $3CdSO_4 \cdot 8H_2O$, supplied by Carlo Erba, were used. A tetramethylammonium hydroxide (TMAH) solution (25%, w/w, electronic grade 99.9999%) supplied by Alfa Aesar® was used. Twice-distilled water prepared in our own laboratory was used in all experiments. Predetermined volumes of $FeCl_3$ and $CdSO_4$ solutions and twice-distilled water were mixed, then TMAH was added as a precipitating agent. The exact experimental conditions for the preparation of samples are given in Table 1. Thus, formed suspensions were vigorously shaken for ∼10 min, then heated at 160 °C, using the Parr general-purpose bomb (model 4744), comprising a teflon vessel and cup. After 2 h of heating the precipitates were cooled to RT (mother liquor pH ∼ 13.5–13.8) and subsequently washed with twice-distilled water using the ultraspeed Sorvall RC2-B centrifuge. After drying, all precipitates were characterised by Mössbauer and FT-IR spectroscopies, as well as high-resolution scanning electron microscopy. The concentrations of iron and cadmium in the particles were determined by EDS analysis.

2.2. Instrumentation

^{57}Fe Mössbauer spectra were recorded in transmission mode using a standard WISSEL GmbH (Starnberg, Germany) instrumental configuration. A ^{57}Co/Rh Mössbauer source was used. The velocity scale and all the data refer to the metallic α-Fe absorber at RT. A quantitative analysis of the recorded spectra was made using the MOSSWINN program.

Fourier transform infrared (FT-IR) spectra were recorded at RT using a Perkin-Elmer spectrometer (model 2000). The FT-IR spectrometer was linked to a PC with an installed IRDM (IR data manager) program to process the recorded spectra. The specimens were pressed into small discs using a spectroscopically pure KBr matrix.

A thermal field emission scanning electron microscope (FE SEM, model JSM-7000F, manufactured by JEOL Ltd.) was used. FE SEM was linked to the EDS/INCA 350 (energy dispersive X-ray analyser) manufactured by Oxford Instruments Ltd. The specimens were not coated with electrically conductive surface layer.

3. Results and discussion

3.1. ^{57}Fe Mössbauer spectroscopy

Reference α-FeOOH (sample G) was precipitated in the highly alkaline medium (pH ∼ 13.5–13.8) using a strong organic alkali (TMAH) as the precipitating agent [1]. Acicular and monodispersed α-FeOOH particles were obtained with a high reproducibility that is important in studying the formation of solid solutions. Adding the TMAH solution to the $FeCl_3$ solution yielded a precipitate (an "amorphous" $Fe(OH)_3$ or the ferrihydrite-like phase) which was completely dissolved at RT with strong shaking, as observed with the naked eye. After a short time of ageing the homogenous recrystallisation of α-FeOOH started.

The Mössbauer spectrum of reference α-FeOOH (sample G) recorded at RT is shown in Fig. 1, whereas the corresponding Mössbauer parameters for this sample are given in Table 2. The spectrum showed a broadening of Mössbauer lines, and the intensities of spectral lines deviated from the theoretical intensity ratio 3:2:1:1:2:3. This spectrum was fitted taking into account hyperfine magnetic field (HMF) distribution as shown in Fig. 1. Generally, the RT Mössbauer spectrum of α-FeOOH may range from a well-shaped sextet to one paramagnetic doublet, depending on the size and crystallinity of α-FeOOH particles. α-FeOOH particles smaller than ∼15–20 nm show a superparamagnetic type of the Mössbauer spectrum at RT, whereas the α-FeOOH particles smaller than 8 nm show a superparamagnetic type of the spectrum down to 77 K [2]. The incorporation of metal cations into the α-FeOOH structure induced a decrease in the average HMF $\langle B_{hf} \rangle$. Reference literature showed varying effects of various metal cations on the formation of solid solutions with α-FeOOH as well as on the size and geometrical shape of the particles. A possible combined effect of poor crystallinity and metal substitution on the Mössbauer spectrum of α-FeOOH was discussed by Murad and Schwertmann [3]. In

Table 1
Experimental conditions for the synthesis of samples G and CG1 to CG8

Sample	2 M $FeCl_3$ (ml)	[$FeCl_3$] (M)	0.1 M $CdSO_4$ (ml)	0.01 M $CdSO_4$ (ml)	[$CdSO_4$] (M)	r = [Cd]/([Cd] + [Fe])	TMAH[a] (ml)	H_2O (ml)
G	2	0.1	–	–	0	0	10	28
CG1	2	0.1	–	4	0.001	0.0099	10	24
CG2	2	0.1	–	8	0.002	0.0196	10	20
CG3	2	0.1	–	12	0.003	0.0291	10	16
CG4	2	0.1	–	16	0.004	0.0385	10	12
CG5	2	0.1	2	–	0.005	0.0476	10	26
CG6	2	0.1	2	4	0.006	0.0566	10	22
CG7	2	0.1	3	–	0.0075	0.0698	10	25
CG8	2	0.1	4	–	0.0100	0.0909	10	24

[a] TMAH, tetramethylammonium hydroxide (25%, w/w).

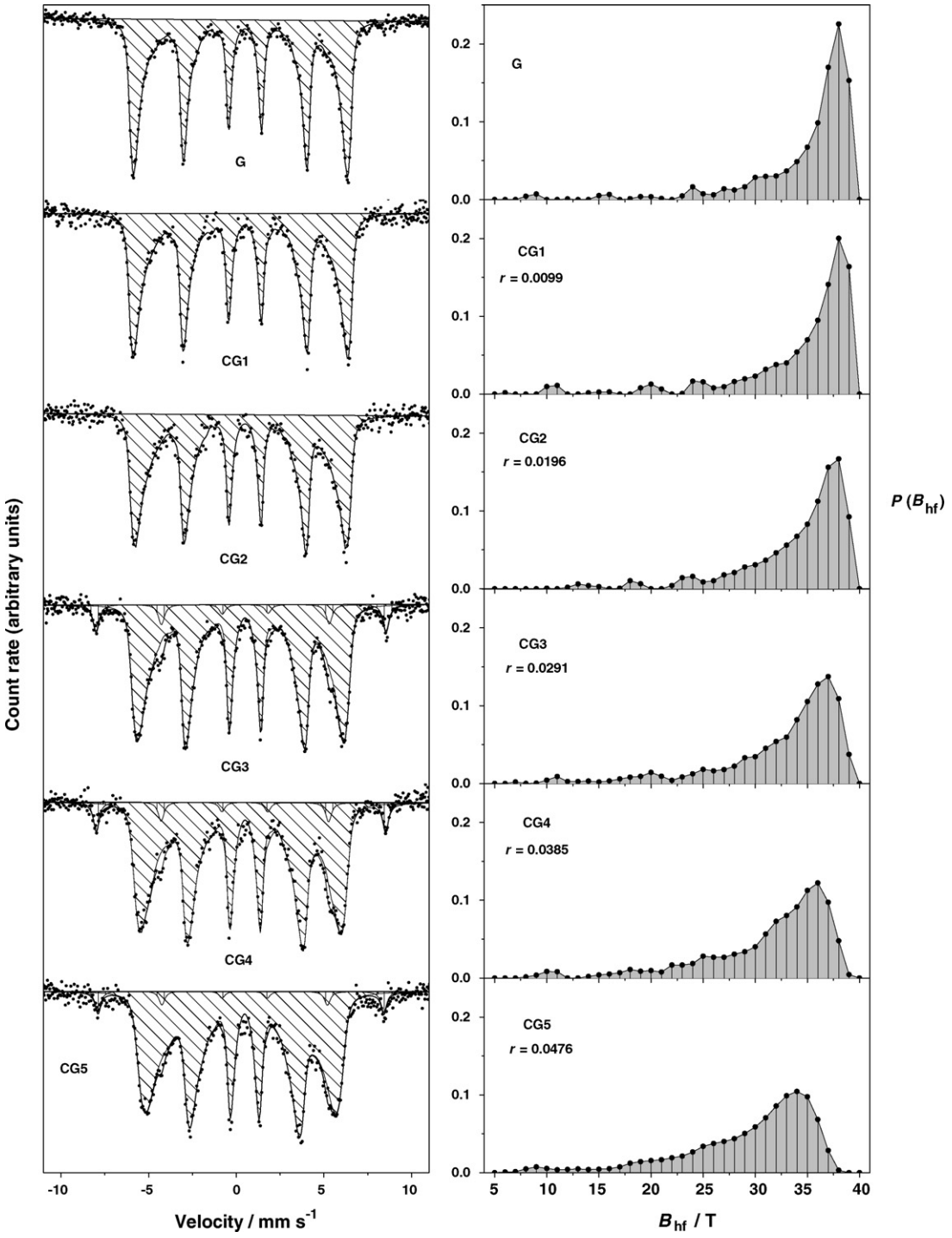

Fig. 1. ^{57}Fe Mössbauer spectra of reference sample G and samples CG1 to CG5, recorded at RT. Corresponding hyperfine magnetic field distributions for α-FeOOH.

the present case the effect of poor crystallinity of α-FeOOH can be neglected. The broadening of spectral lines and the decrease of $\langle B_{hf} \rangle$ can be assigned to the effect of Cd-substitution in the α-FeOOH structure.

At the concentration ratio up to $r = [Cd]/([Cd] + [Fe]) = 0.0196$ an α-FeOOH type structure alone was obtained with a $\langle B_{hf} \rangle$ decreased from 34.9 to 34.0 T. In the range $r = 0.0291$–0.0476 an α-Fe_2O_3 type structure was additionally present. The content of this phase slightly changed from 7.9 to 5.8% with the corresponding change in $\langle B_{hf} \rangle$ from 51.3 to 50.8 T. This decrease in the B_{hf} value in relation to 51.8 T recorded for an undoped α-Fe_2O_3 [4] can be assigned to the incorporation of Cd^{2+} ions into the α-Fe_2O_3 structure. Fig. 1 also shows a broadening of the HMF distributions and a shift of the most probable HMF with an increased r. Fig. 2 shows the RT Mössbauer spectra of samples CG6 to CG8 ($r = 0.0566$–0.0909). The amount of the α-$(Fe, Cd)_2O_3$ phase in sample CG6 significantly increased (22.2%), whereas in samples CG7 and CG8 the α-$(Fe, Cd)_2O_3$

Table 2
Fe Mössbauer parameters calculated for samples G and CG1 to CG8 and identification

Sample	Spectral line	δ (mm s^{-1})	E_q or Δ (mm s^{-1})	B_{hf} (T)	Γ (mm s^{-1})	Area (%)	Identification
G	M	0.37	−0.26	34.9	0.28	100	α-FeOOH
CG1	M	0.37	−0.26	34.3	0.31	100	α-(Fe, Cd)OOH
CG2	M	0.37	−0.25	34.0	0.27	100	α-(Fe, Cd)OOH
CG3	M_1	0.37	−0.26	32.6	0.28	92.1	α-(Fe, Cd)OOH
	M_2	0.39	−0.24	51.3	0.41	7.9	α-(Fe, Cd)$_2$O$_3$
CG4	M_1	0.38	−0.25	31.3	0.31	92.8	α-(Fe, Cd)OOH
	M_2	0.38	−0.22	51.2	0.39	7.2	α-(Fe, Cd)$_2$O$_3$
CG5	M_1	0.37	−0.25	29.7	0.31	94.2	α-(Fe, Cd)OOH
	M_2	0.40	−0.18	50.8	0.44	5.8	α-(Fe, Cd)$_2$O$_3$
CG6	M_1	0.38	−0.23	30.5	0.30	77.8	α-(Fe, Cd)OOH
	M_2	0.38	−0.21	50.8	0.26	22.2	α-(Fe, Cd)$_2$O$_3$
CG7	M	0.38	−0.21	51.1	0.24	100	α-(Fe, Cd)$_2$O$_3$
CG8	M	0.38	−0.21	50.8	0.24	100	α-(Fe, Cd)$_2$O$_3$

Errors: $\delta = \pm 0.01$ mm s^{-1}, $E_q = \pm 0.01$ mm s^{-1}, $B_{hf} = \pm 0.2$ T. Isomer shift is given relative to α-Fe.

phase alone was found by Mössbauer spectroscopy. Since there was no significant change in B_{hf} values, nor in Γ values, it can be concluded that in these samples the incorporation of Cd^{2+} into the α-Fe_2O_3 structure was maximal. The HMF distributions calculated for α-(Fe, Cd)$_2$O$_3$, shown in Fig. 2, are in line with the previous conclusion. Fig. 3 illustrates the dependence of the average hyperfine magnetic field in α-FeOOH and α-Fe_2O_3 on the [Cd]/([Cd] + [Fe]) ratio (r). The reference hyperfine magnetic fields of 34.9 T for reference α-FeOOH [1] and 51.8 T [4] for α-Fe_2O_3 were used.

Other researchers used alternative methods to Mössbauer spectroscopy in their studies about the influence of Cd^{2+} on the precipitation of *iron oxides* and the formation of solid solutions. For example, Martinez and McBride [5] investigated the influence of Cd^{2+}, Cu^{2+}, Pb^{2+} and Zn^{2+} ions on the transformation of the corresponding ferrihydrite coprecipitate. The thermal treatment of coprecipitates reduced the solubility of Cd^{2+} and Zn^{2+} ions, Pb^{2+} ions were almost removed from the precipitate, whereas the coprecipitate with Cu^{2+} ions was the most stable, which was explained by the structural incorporation of Cu^{2+} ions

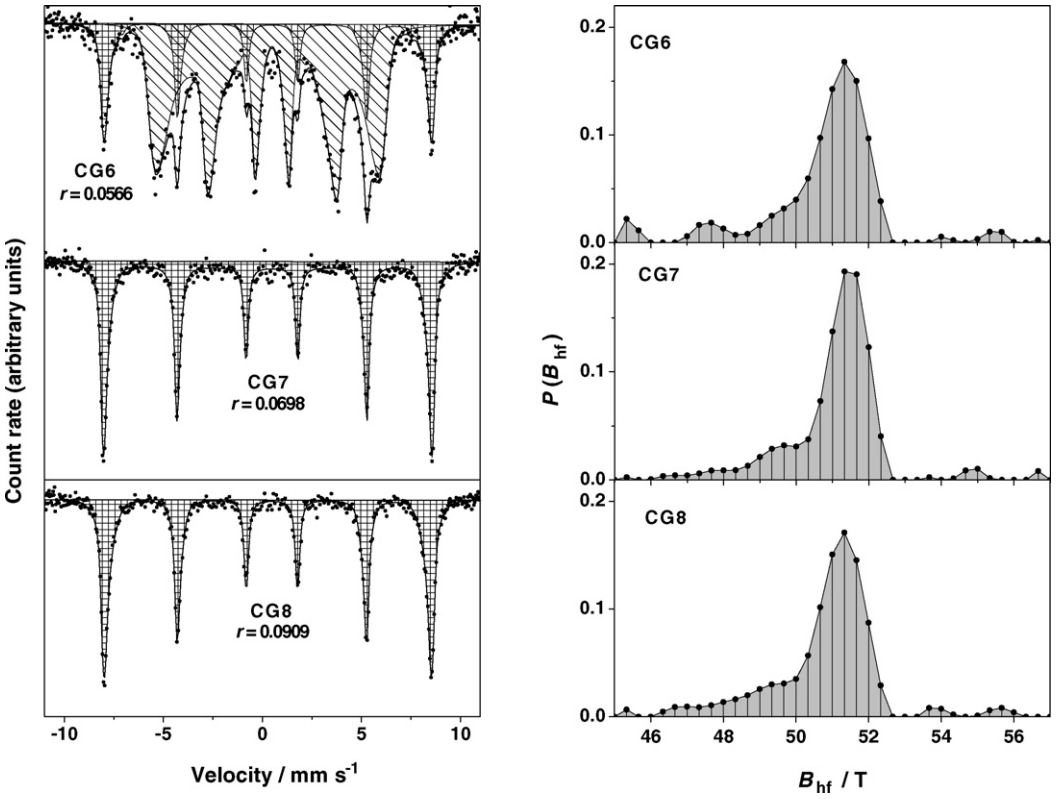

Fig. 2. ^{57}Fe Mössbauer spectra of samples CG6 to CG8, recorded at RT. Corresponding hyperfine magnetic field distributions for α-Fe_2O_3.

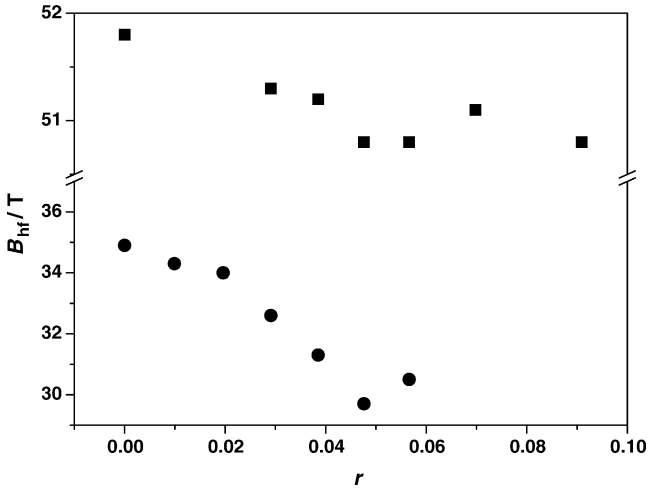

Fig. 3. Dependence of the average hyperfine magnetic field in α-FeOOH (●) and α-Fe_2O_3 (■) on the [Cd]/([Cd] + [Fe]) ratio (r).

into the host matrix. It was suggested that initial coprecipitate products determined the final thermal transformation products. In these transformations, ferrihydrite, hematite, goethite and lepidocrocite (γ-FeOOH) were detected. Lin et al. [6] investigated the effect of cadmium(II) on the transformation of ferrihydrite in neutral and alkaline media (pH 7–11). They concluded that the presence of Cd(II) strongly retards the transformation of ferrihydrite into hematite and goethite, and enhances the formation of hematite relative to goethite. About 2.5 mol% of Cd(II) was included in the hematite structure for an initial 5 mol% addition of Cd(II). At pH 11 the presence of Cd(II) led to a reduction in size and enhanced the twinning of goethite crystals. Huynh et al. [7] found that about 10 mol% of Cd^{2+} could be incorporated into α-FeOOH in octahedral sites. XRD data were refined by the Rietveld method. A progressive increase in the values of unit-cell parameters was influenced by a great difference in the ionic radii of Cd^{2+} (0.95 Å) and Fe^{3+} (0.645 Å). On the basis of TEM observations the authors have also reported that the particle size decreased with an increased Cd-substitution. Sileo et al. [8] prepared Cd-substituted α-FeOOH samples by precipitation in alkaline media. The authors used the Rietveld analysis of XRD data and reported that the α-FeOOH structure was preserved up to $\mu_{Cd} = 5.50$, where $\mu_{Cd} = [Cd] \times 100/([Cd] + [Fe])$. The incorporation of Cd^{2+} ions into the α-FeOOH structure was drastically reduced at $\mu_{Cd} = 7.03$, and it was suggested that for the same μ_{Cd} value a Cd-substituted α-Fe_2O_3 was formed as an associated phase. The authors observed acicular habits of α-FeOOH particles of varying lengths, whereas α-(Fe, Cd)OOH particles up to $\mu_{Cd} = 5.50$ also contained star-shaped twins. The length-to-width ratio increased upon cadmium incorporation, and the largest ratio (∼12) was found for $\mu_{Cd} = 3.63$. For $\mu_{Cd} = 7.03$, the authors observed a drastic decrease in the length of α-(Fe, Cd)OOH needles and in the population of star-shaped particles. Gerth [9] used XRD to measure the unit-cell dimensions of the M-substituted α-FeOOH (M = Co^{3+}, Ni^{2+}, Cu^{2+}, Zn^{2+}, Cd^{2+} or Pb^{4+}). These samples were prepared under highly alkaline conditions. The author found that changes in the b-dimension of M-substituted α-FeOOH per unit mol% incorporation could be linearly related to the ionic radii of the

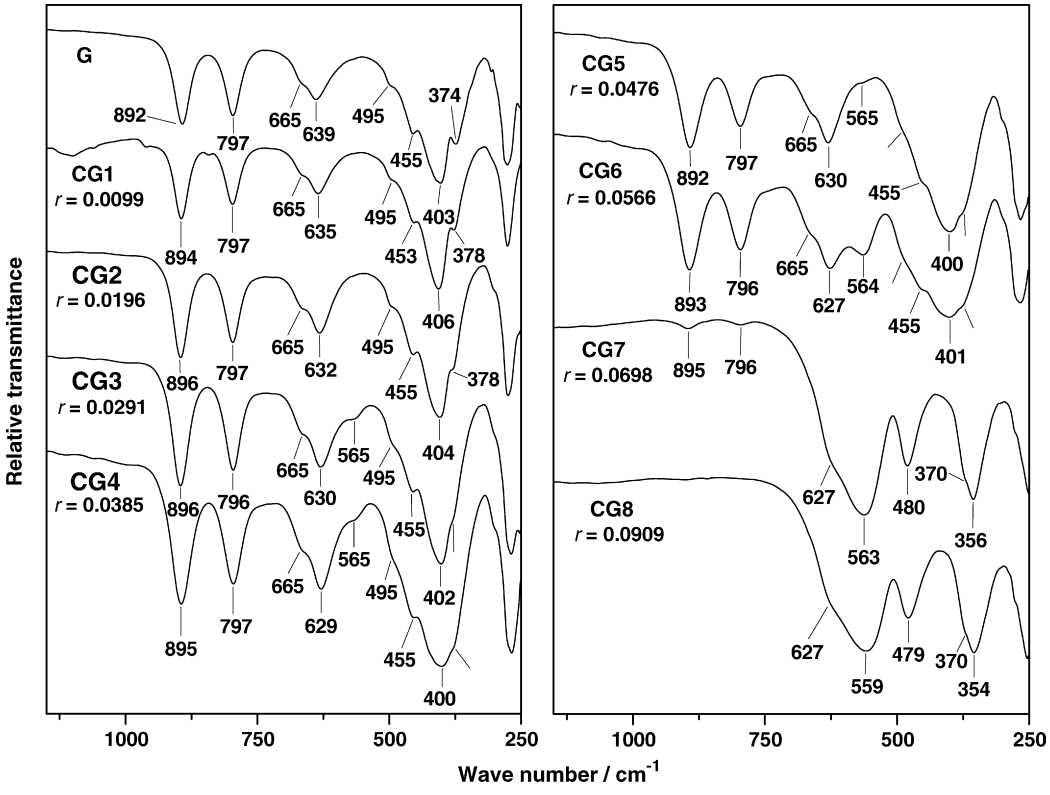

Fig. 4. FT-IR spectra of sample G and samples CG1 to CG8 recorded at RT.

M-substitutions. For Cd^{2+}, the linearity of *b*-dimension was observed up to ~5 mol% substitution, whereas for *a*-dimension this linearity was observed up to ~2 mol%.

Incorporations of metal cations with the charges different than three into the α-FeOOH or α-Fe_2O_3 structure change the electrical neutrality in the corresponding crystal lattice. For example, zinc K-edge EXAFS and interatomic potential calculations indicated that Zn^{2+} ions made solid solutions with α-Fe_2O_3 and that the charge balance is achieved by oxygen vacancies [10]. Berry et al. [11] suggested that Sn^{4+}, Ti^{4+} and Mg^{2+} occupy both interstitial and substitutional sites in the α-Fe_2O_3 related structure. Carvalho-e-Silva et al. [12] suggested that the Fe^{3+} for Ni^{2+} substitution in α-FeOOH can be explained by a mechanism which includes the compensation of the charge imbalance in crystal lattice. According to this model, the Fe^{3+} for Ni^{2+} substitution is accompanied by a proton capture resulting in $NiO_2(OH)_4$ octahedra. In the present case, we suggest that Cd^{2+} ions with great ionic radii (0.95 Å) substitute Fe^{3+} ions in the α-Fe_2O_3 type structure and strongly distort this structure, whereas the oxygen vacancies formed serve for compensation of the charge imbalance. On the other hand, in the case of Cd-substituted α-FeOOH there is possibility of: (a) proton capture for the compensation of the electric charge in this structure or (b) mixed effect which includes proton capture, as well as counter charge of the crystal defects (oxygen vacancies).

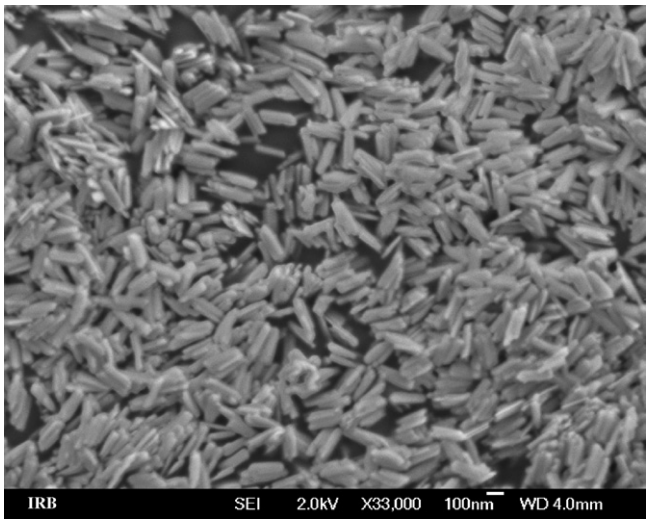

Fig. 5. FE SEM micrograph of reference α-FeOOH (sample G).

3.2. FT-IR spectroscopy

The characteristic parts of the FT-IR spectra of sample G and samples CG1 to CG8 are shown in Fig. 4. The corresponding *r* values are also denoted. The spectrum of sample G corresponds

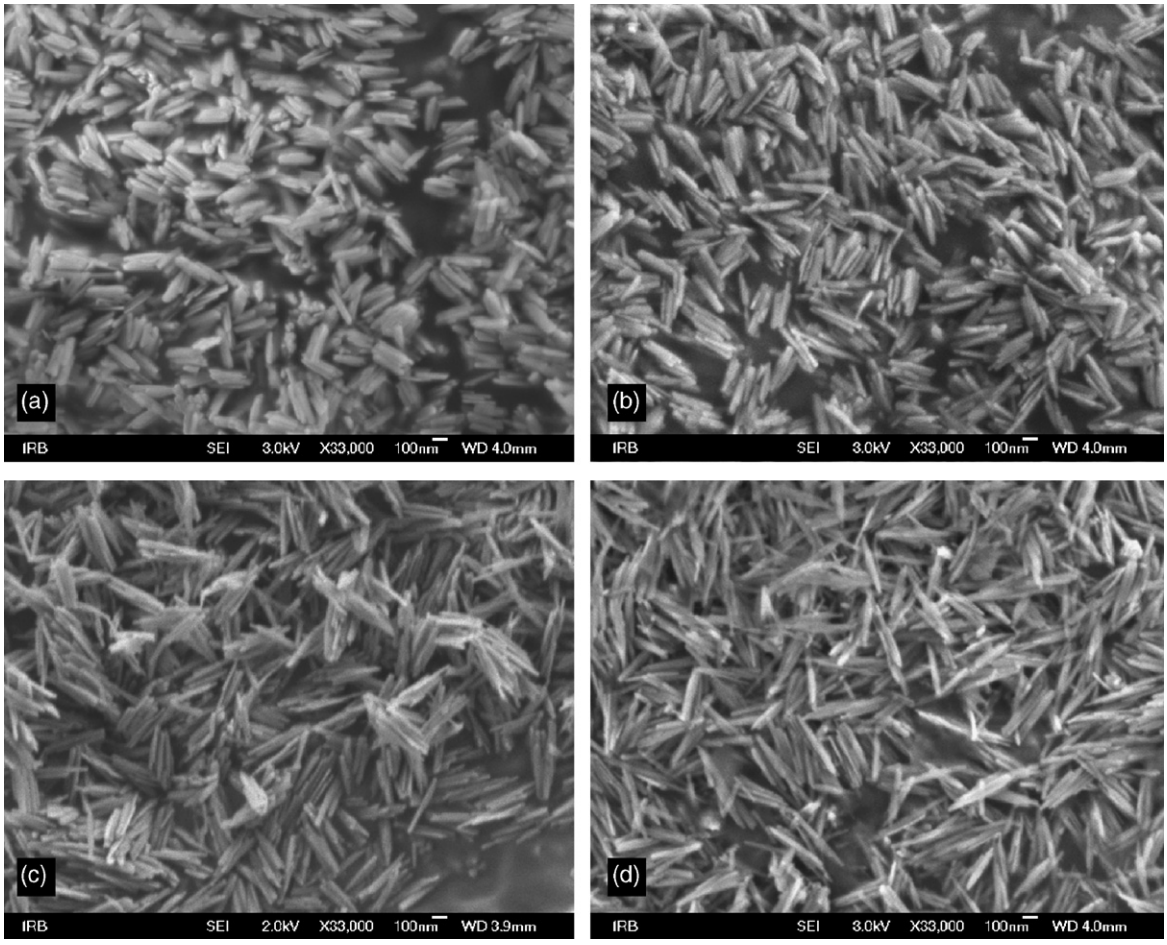

Fig. 6. FE SEM micrographs of samples: (a) CG1, (b) CG2, (c) CG3 and (d) CG4.

to a pure α-FeOOH. Two typical IR bands of α-FeOOH at 892 and 797 cm^{-1} can be assigned to Fe–O–H bending vibrations. Verdonck et al. [13] applied the method of normal coordinate analysis to the study of the IR spectrum of α-FeOOH, and also compared experimental and calculated vibrational frequencies of α-FeOOH and α-FeOOD. The IR bands recorded at 630, 495 and 270 cm^{-1} were rather insensitive to deuteration, hence they were assigned to Fe–O stretching vibrations. Cambier [14] also investigated the IR spectrum of α-FeOOH in line with that of Verdonck et al. [13]. The author also reported that an intense IR band around 630 cm^{-1} was influenced by the geometrical shape of the α-FeOOH particles. The incorporation of Cd^{2+} ions into the α-FeOOH structure influenced the IR band at 639 cm^{-1} and a shift to 632 cm^{-1} was observed in sample CG2. With a further increase in *r* there was a gradual shift of this IR band to lower wave numbers, while in sample CG6 it was located at 627 cm^{-1}. The spectrum of sample CG3 showed a shoulder at 565 cm^{-1} which could be assigned to the α-Fe_2O_3 structure, taking into account the Mössbauer results, whereas in sample CG6 the intensity of this band at 564 cm^{-1} significantly increased, in conformity with the Mössbauer phase analysis (Table 2). The IR spectra of samples CG7 and CG8 correspond to the α-Fe_2O_3 phase or, more precisely, to α-(Fe, Cd_2)O_3. The IR bands at 895 and 796 cm^{-1}, observed in sample CG7, can be assigned to a small amount of α-(Fe, Cd)OOH particles. FT-IR spectroscopy is a specifically important technique in the determination of small or trace amounts of α-FeOOH or γ-FeOOH in samples. The FT-IR spectrum of sample CG8 [α-(Fe, Cd_2)O_3] is characterised by three dominant IR bands at 559, 479 and 354 cm^{-1}, as well as two shoulders at 627 and 370 cm^{-1}. Iglesias and Serna [15] reported the IR spectra of α-Fe_2O_3 particles of different geometrical shapes. α-Fe_2O_3 spheres showed IR bands at 575, 485, 385 and 360 cm^{-1}, whereas α-Fe_2O_3 laths showed IR bands at 650, 525, 440 and 300 cm^{-1}.

3.3. FE SEM

Fig. 5 shows an FE SEM micrograph of undoped acicular α-FeOOH particles [1] which were used as reference material in the present investigation. With an increased Cd-substitution the elongation of α-FeOOH particles along the *c*-axis is well visible (Fig. 6: samples CG1 to CG4). This effect can be assigned to the formation of α-(Fe, Cd)OOH solid solutions upon Cd-substitutions in octahedral sites. The elongation of α-(Fe, Cd)OOH particles could be also enhanced by the preferential adsorption of Cd^{2+} ions along the *c*-axis. The adsorption of metal cations on iron oxides increases with an increased pH [16], whereas pH-dependence of the adsorption of oxyanions

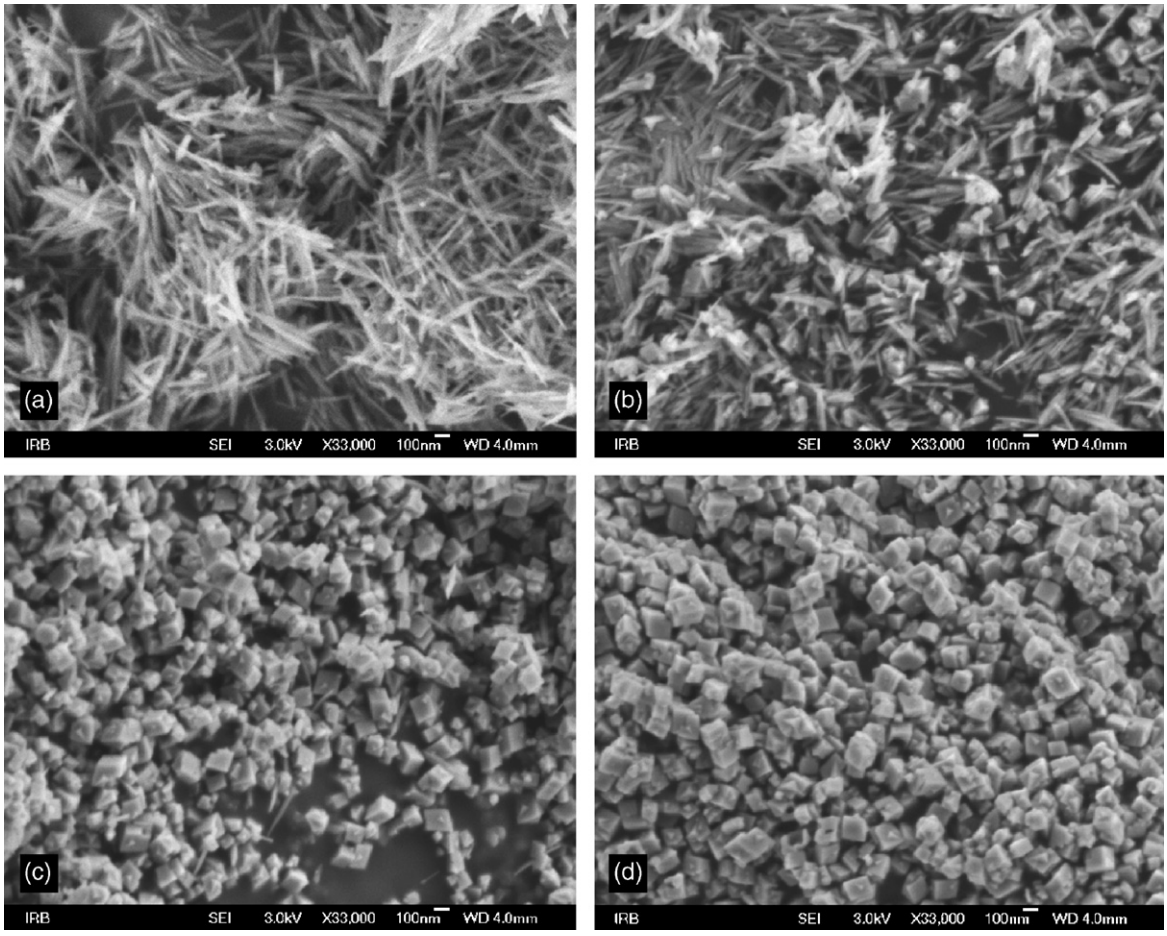

Fig. 7. FE SEM micrographs of samples: (a) CG5, (b) CG6, (c) CG7 and (d) CG8.

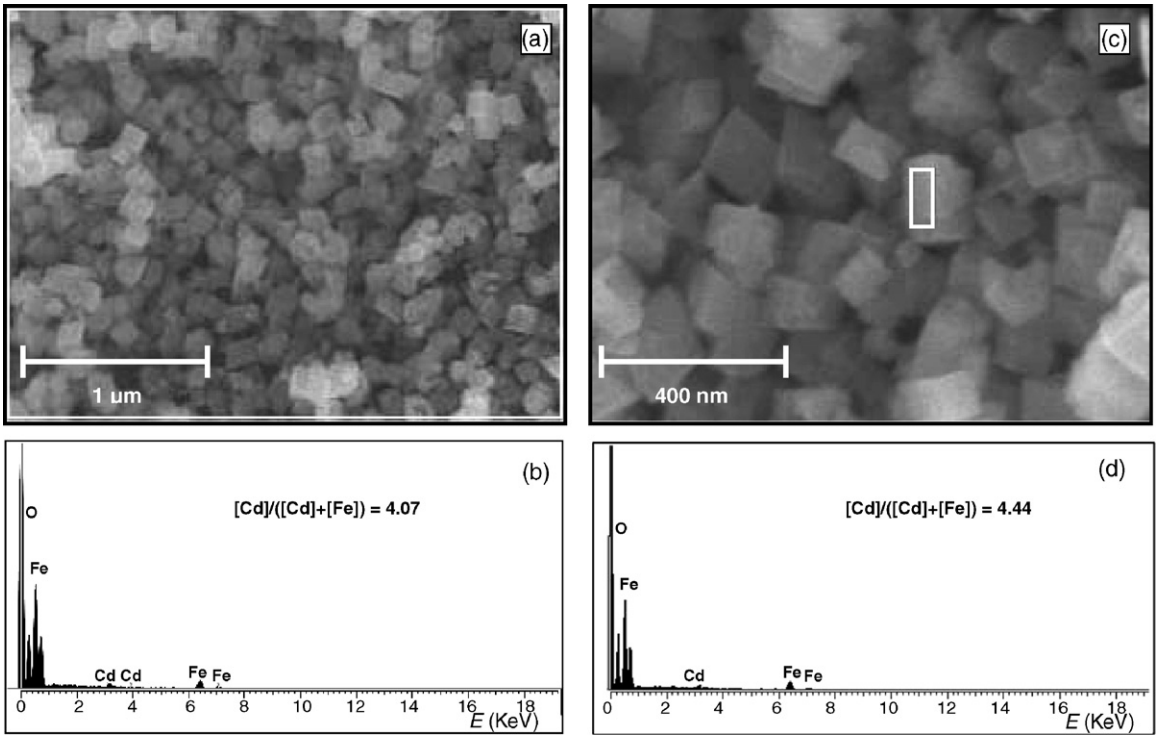

Fig. 8. EDS analyses of sample CG8: (a and b) total screen and (c and d) detail on the surface of one α-(Fe, Cd_2)O_3 particle.

is in opposite direction [17]. However, in the present case the predominant influence on the elongation of α-FeOOH particles along the *c*-axis is the formation of solid solutions, as mentioned earlier. Specifically adsorbed sulphates may also enhance the elongation of *iron oxide* particles. In the present work, Cd^{2+} ions were dissolved in a sulphate form; however, sulphates were not detected in CG samples by FT-IR spectroscopy, which is generally a technique very sensitive to specifically adsorbed sulphates [18].

Fig. 7 shows the FE SEM micrographs of samples CG5 to CG8. A gradual increase in the length of α-(Fe, Cd)OOH particles from sample CG1 (∼250–300 nm) to CG5 (∼600–700 nm) was observed. At the same time, particle width (*b*-axis direction) and thickness (*a*-axis direction) showed a gradual decrease, and in this way the rod-like α-FeOOH particles in reference sample (Fig. 5) became long and thin needle-like particles (Fig. 7a) upon increased cadmium substitution. Sample CG6 showed a decrease in the length of α-(Fe, Cd)OOH particles (∼400–500 nm), whereas a very small fraction of α-(Fe, Cd)OOH particles (∼250–400 nm) was obtained in sample CG7. Sample CG5 showed small α-(Fe, $Cd)_2O_3$ particles of ∼100 nm or less. α-(Fe, $Cd)_2O_3$ particles gradually increased, while in sample CG8 their size was ∼100–200 nm. Fig. 8 shows an EDS analysis of sample CG8; (a and b) total screen and (c and d) detail on the surface of one α-(Fe, $Cd)_2O_3$ particle. Taking into account that the size of α-(Fe, $Cd)_2O_3$ particles is greater than that of superparamagnetic α-Fe_2O_3 particles, and that these particles are not poor crystalline, it can be inferred that the decreased $\langle B_{hf} \rangle$ value is a direct consequence of the incorporation of Cd^{2+} ions into the α-Fe_2O_3 structure.

4. Conclusion

- Acicular and monodisperse α-FeOOH particles were prepared in highly alkaline media (pH ∼ 13.5–13.8) using the procedure given by Krehula et al. [1]. These particles were used as reference material in the investigation of the effect of Cd^{2+} ions on the phenomenology of the precipitation of α-(Fe, Cd)OOH and α-(Fe, $Cd)_2O_3$ particles in highly alkaline media, the formation of solid solutions, as well as on the size and geometrical shape of the particles produced.
- The $\langle B_{hf} \rangle$ value of the hyperfine magnetic field in α-FeOOH was decreasing upon the incorporation of Cd^{2+} ions into the α-FeOOH structure. An α-(Fe, Cd)OOH solid solution was alone obtained up to $r = 0.0196$, where $r = [Cd]/([Cd] + [Fe])$. Mössbauer spectroscopy showed the formation of two phases at *r* values between 0.0291 and 0.0566, corresponding to α-(Fe, Cd)OOH and α-(Fe, $Cd)_2O_3$ solid solutions. In addition to this, FT-IR spectroscopy and FE SEM showed a very small amount of α-(Fe, Cd)OOH particles, beside α-(Fe, $Cd)_2O_3$ particles, in a sample with $r = 0.0698$. At $r = 0.0909$ the precipitation system yielded only α-(Fe, $Cd)_2O_3$ particles. The $\langle B_{hf} \rangle$ values in α-(Fe, $Cd)_2O_3$ also decreased upon an increased incorporation of Cd^{2+} ions into the α-Fe_2O_3 structure. FT-IR spectroscopy monitored qualitatively the formation of α-FeOOH and α-Fe_2O_3 phases in the samples. The IR band at 639 cm^{-1} observed in sample G was the one most sensitive to Cd-substitution in an α-FeOOH structure, and it shifted to 627 cm^{-1} in sample CG6 ($r = 0.0566$).
- With an increased *r* value, a gradual elongation of α-(Fe, Cd)OOH particles in the *c*-axis direction along with a decreased

width (*b*-axis direction) and thickness (*a*-axis direction) was observed. The maximum elongation (∼600–700 nm) was obtained in sample CG5 ($r = 0.0476$), and with a further increase in the r value (samples CG6 and CG7), the length of α-(Fe, Cd)OOH particles rapidly decreased. At $r = 0.0909$ (sample CG8), FE SEM showed well defined α-$(Fe, Cd)_2O_3$ particles, ∼100–200 nm in size.

References

[1] S. Krehula, S. Popović, S. Musić, Mater. Lett. 54 (2002) 108–113.
[2] E. Murad, J.H. Johnston, in: G.J. Long (Ed.), Iron Oxides and Oxyhydroxides in Mössbauer Spectroscopy Applied to Inorganic Chemistry, vol. 2, Plenum Publishing Corporation, 1987, pp. 507–582.
[3] E. Murad, U. Schwertmann, Clay Miner. 18 (1983) 301–312.
[4] S. Musić, I. Czakó-Nagy, S. Popović, A. Vértes, M. Tonković, Croat. Chem. Acta 59 (1986) 833–851.
[5] C.E. Martinez, M.B. McBride, Clays Clay Miner. 46 (1998) 537–545.
[6] X. Lin, R.C. Burns, G.A. Lawrance, Water Air Soil Pollut. 143 (2003) 155–177.
[7] T. Huynh, A.R. Tong, B. Singh, B.J. Kennedy, Clays Clay Miner. 51 (2003) 397–402.
[8] E.E. Sileo, P.S. Solís, C.O. Paiva-Santos, Powder Diffr. 18 (2003) 50–55.
[9] J. Gerth, Geochim. Cosmochim. Acta 54 (1990) 363–371.
[10] I. Ayub, F.J. Berry, R.L. Bilsborrow, Ö. Helgason, R.C. Mercader, E.A. Moore, S.J. Stewart, P.G. Wynn, J. Solid State Chem. 156 (2001) 408–414.
[11] F.J. Berry, C. Greaves, Ö. Helgason, J. McManus, H.M. Palmer, R.T. Williams, J. Solid State Chem. 151 (2000) 157–162.
[12] M.L. Carvalho-e-Silva, A.Y. Ramos, H.C.N. Tolentino, J. Enzweiler, S.M. Netto, M. Do Carmo Martins Alves, Am. Miner. 88 (2003) 876–882.
[13] L. Verdonck, S. Hoste, F.F. Roelandt, G.P. Van der Kelen, J. Mol. Struct. 79 (1982) 273–279.
[14] P. Cambier, Clay Miner. 21 (1986) 191–200.
[15] J.E. Iglesias, C.J. Serna, Miner. Petrogr. Acta 29A (1985) 365.
[16] S. Musić, M. Ristić, J. Radioanal. Nucl. Chem. 120 (1988) 289–304.
[17] S. Musić, M. Ristić, M. Tonković, Z. Wasser-Abwasser-Forsch. 19 (1986) 186–196.
[18] S. Musić, A. Šarić, S. Popović, K. Nomura, T. Sawada, Croat. Chem. Acta 73 (2000) 541–567.